Clinical Cancer Research

Comprehensive Genomic Profiling Identifies Novel Genetic Predictors of Response to Anti–PD-(L)1 Therapies in Non–Small Cell Lung Cancer

Wenfeng Fang[1], Yuxiang Ma[1], Jiani C. Yin[2], Shaodong Hong[1], Huaqiang Zhou[1], Ao Wang[3], Fufeng Wang[2], Hua Bao[3], Xue Wu[3], Yunpeng Yang[1], Yan Huang[1], Hongyun Zhao[1], Yang W. Shao[2,4], and Li Zhang[1]

Abstract

Purpose: Immune checkpoint inhibitors (ICI) have revolutionized cancer management. However, molecular determinants of response to ICIs remain incompletely understood.

Experimental Design: We performed genomic profiling of 78 patients with non–small cell lung cancer (NSCLC) who underwent anti–PD-(L)1 therapies by both whole-exome and targeted next-generation sequencing (a 422-cancer-gene panel) to explore the predictive biomarkers of ICI response. Tumor mutation burden (TMB), and specific somatic mutations and copy-number alterations (CNA) were evaluated for their associations with immunotherapy response.

Results: We confirmed that high TMB was associated with improved clinical outcomes, and TMB quantified by gene panel strongly correlated with WES results (Spearman's $\rho = 0.81$). Compared with wild-type, patients with *FAT1* mutations had higher durable clinical benefit (DCB, 71.4% vs. 22.7%, $P = 0.01$) and objective response rates (ORR, 57.1% vs. 15.2%, $P = 0.02$). On the other hand, patients with activating mutations in *EGFR*/*ERBB2* had reduced median progression-free survival (mPFS) compared with others [51.0 vs. 70.5 days, $P = 0.0037$, HR, 2.47; 95% confidence interval (CI), 1.32–4.62]. In addition, copy-number loss in specific chromosome 3p segments containing the tumor-suppressor *ITGA9* and several chemokine receptor pathway genes, were highly predictive of poor clinical outcome (survival rates at 6 months, 0% vs. 31%, $P = 0.012$, HR, 2.08; 95% CI, 1.09–4.00). Our findings were further validated in two independently published datasets comprising multiple cancer types.

Conclusions: We identified novel genomic biomarkers that were predictive of response to anti–PD-(L)1 therapies. Our findings suggest that comprehensive profiling of TMB and the aforementioned molecular markers could result in greater predictive power of response to ICI therapies in NSCLC.

Introduction

Immune checkpoint inhibitors (ICI) have demonstrated remarkable clinical activity against a multitude of advanced cancers (1), yet response and durable clinical benefit are only achieved in a small subset of patients (2). Tumor expression of programmed death-ligand 1 (PD-L1) is the first FDA-approved predictive biomarker for ICI treatment (3), followed by microsatellite instability (MSI) status and mismatch repair deficiency (dMMR; ref. 4). However, none of these biomarkers can fully capture the pattern of response to anti-programmed cell death protein-1 (PD-1) or anti–PD-L1 (hereafter, anti–PD-(L)1) therapies. The objective response rates (ORRs) in non–small cell lung cancer (NSCLC) were less than 50% regardless of PD-L1 status of the tumors (5–12). Tumor mutation burden (TMB), a potential indicator of tumor immunogenicity, is an emerging predictive biomarker of response to ICI treatments independent of PD-L1 expression. Numerous studies have demonstrated a strong association between TMB levels and clinical outcomes in various tumor types, including lung cancers (8, 13–18). However, similar to PD-L1 expression, TMB is not perfectly correlated with ICI response and shows substantially overlapping distribution between responders and non-responders with reported ORRs of 30% to 50% for TMB-high patients (17, 19). A number of studies have suggested other potential biomarkers, including tumor clonality (20), somatic mutations in specific genes (21), and copy-number alterations (CNA) affecting genes and signaling pathways with important immune-related functions (22, 23). Nevertheless, many of these biomarkers are specific to certain cancer types or patient cohorts. Therefore, identification of additional biomarkers with greater predictive value for the efficacy of ICI therapy, especially those that are robust across different cancer types and patient populations, is crucial in assisting treatment decision-making.

[1]State Key Laboratory of Oncology in South China, Collaborative Innovation Center for Cancer Medicine, Sun Yat-sen University Cancer Center, Guangzhou, Guangdong, China. [2]Nanjing Geneseeq Technology Inc., Nanjing, Jiangsu, China. [3]Geneseeq Technology Inc., Toronto, Ontario, Canada. [4]School of Public Health, Nanjing Medical University, Nanjing, Jiangsu, China.

Note: Supplementary data for this article are available at Clinical Cancer Research Online (http://clincancerres.aacrjournals.org/).

W. Fang, Y. Ma, J.C. Yin, S. Hong contributed equally to this article.

Corresponding Authors: Li Zhang, Sun Yat-sen University Cancer Center, Guangzhou, Guangdong, 510060, 510060. Phone: 86-208-734-3458; E-mail: zhangli6@mail.sysu.edu.cn; Wenfeng Fang, fangwf@sysucc.org.cn; and Yang W. Shao, yang.shao@geneseeq.com

Clin Cancer Res 2019;25:5015–26

doi: 10.1158/1078-0432.CCR-19-0585

Translational Relevance

Despite the notable successes of immune checkpoint inhibitors (ICI), the majority (over 80%) of unselected patients failed to derive durable clinical benefit. Given the complex interactions between tumors and the immune system, it is conceivable that multiple biomarkers are necessary to distinguish responders and nonresponders. We performed comprehensive genomic profiling of 78 non–small cell lung cancer (NSCLC) patients who underwent anti–PD-(L)1 treatments by both whole-exome and targeted sequencing. In addition to validation of tumor mutation burden (TMB) as a predictive biomarker for clinical outcomes, we identified novel genomic features that jointly with TMB refine the prediction of patients' response to immunotherapy. Specifically, *FAT1* mutations correlated with responsiveness to therapy, whereas mutations in *EGFR/ERBB2* and loss of chemokine receptor pathway genes and specific chromosome 3p segments predicted poor clinical outcome. Our findings were further validated in two independently published datasets comprising multiple cancer types, and should be of great clinical relevance and significance.

Here, we performed genomic profiling of pre-treatment primary tumors from a cohort of 78 Chinese patients with NSCLC underwent anti–PD-(L)1 therapies, by both whole-exome sequencing (WES) and targeted next-generation sequencing (NGS) using a customized 422-cancer-gene panel (Geneseeq). TMB, specific recurrent somatic mutations and CNAs were analyzed for their correlations to patients' durable clinical response (DCB) and progression-free survival (PFS). In addition to TMB, *EGFR/ERBB2* activating mutations and *FAT1* mutations, as well as CNAs in specific chromosome 3p segments containing tumor-suppressor and chemokine receptor pathway genes were identified as strong predictive biomarkers of response to immune checkpoint blockade. These results were further validated in two independent datasets encompassing both NSCLC and other cancer types, indicating that these biomarkers are robust in predicting the efficacy of immunotherapy.

Materials and Methods

Patients and response assessment

The patients with NSCLC in this study were treated with anti–PD-(L)1 monotherapy agents at Sun Yat-sen University Cancer Center between December 2015 (the first date on which a patient with NSCLC was treated) and August 2017 (the last date to have begun therapy), data cutoff value in January 2019. All patients were treated as part of clinical trials. Eligible patients for this study were determined based on the following criteria: (i) be >18 years old; (ii) Eastern Cooperative Oncology Group performance status: 0–1; (iii) have advanced or recurrent NSCLC; (iv) failure after first-line platinum-based doublets chemotherapy; (v) radiologically evaluable according to Response Evaluation Criteria in Solid Tumors (RECIST) version 1.1. Computed tomography (CT) or magnetic resonance imaging (MRI) scans were reviewed by the investigators. The median follow-up time was 637 days. Progression-free survival (PFS) was defined as the time from the beginning of treatment to the date of progression disease (PD). Patients who had not progressed were censored at the date of their last scan. Objective response rate was defined as the percentage of patients with complete response (CR) or partial response (PR). Durable clinical benefit (DCB) was defined as the percentage of patients who achieved CR or PR or stable disease (SD) lasted >6 months; non-durable clinical benefit (NDB) was defined as PD or SD that lasted $\leq$6 months. The study was conducted in accordance with declaration of Helsinki, and was approved by the Ethical Review Board of Sun Yat-sen University Cancer Center. Informed written consent was obtained from each subject or each subject's guardian.

Library preparation and sequencing

For WES, genomic DNAs from FFPE sections or biopsy samples and the whole blood control samples were extracted with QIAamp DNA FFPE Tissue Kit and DNeasy Blood and tissue kit (Qiagen), respectively, and quantified by Qubit 3.0 using the dsDNA HS Assay Kit (ThermoFisher Scientific). Library preparations were performed with KAPA Hyper Prep Kit (KAPA Biosystems). Target enrichment was performed using the xGen Exome Research Panel and Hybridization and Wash Reagents Kit (Integrated DNA Technology) according to the manufacturer's protocol. Sequencing was performed on Illumina HiSeq4000 platform using PE150 sequencing chemistry (Illumina).

For targeted-panel, customized xGen lockdown probes (Integrated DNA Technologies) targeting 422 cancer-relevant genes were used for hybridization enrichment. The capture reaction was performed with Dynabeads M-270 (Life Technologies) and xGen Lockdown hybridization and wash kit (Integrated DNA Technologies) according to the manufacturers' protocols. Captured libraries were on-beads PCR amplified with Illumina p5 (5′ AAT GAT ACG GCG ACC ACC GA 3′) and p7 primers (5′ CAA GCA GAA GAC GGC ATA CGA GAT 3′) in KAPA HiFi HotStart ReadyMix (KAPA Biosystems), followed by purification using Agencourt AMPure XP beads. Libraries were quantified by qPCR using KAPA Library Quantification kit (KAPA Biosystems). Library fragment size was determined by Bioanalyzer 2100 (Agilent Technologies). The target-enriched library was then sequenced on HiSeq4000 or HiSeq4000 NGS platforms (Illumina) according to the manufacturer's instructions.

The average coverage depth was 140X and 1341X for tumors (64X and 143X in normal blood controls) using WES and Panel, respectively. The average coverage size of WES and Panel for TMB estimation was 32 Mb and 1.4 Mb, respectively.

Mutation calling

Trimmomatic was used for FASTQ file quality control. Leading/trailing low quality (quality reading below 20) or N bases were removed. Paired-end reads were then aligned to the reference human genome (build hg19), using the Burrows–Wheeler Aligner (BWA) with the parameters. PCR deduplication was performed using Picard and local realignment around indels and base quality score recalibration were performed using GATK3. Matched tumor and normal sample pairs were first checked to have the same SNP fingerprint using VCF2LR (GeneTalk) and nonmatching samples were removed from analysis. Further, samples with mean dedup depth <30X were removed. Cross-sample contamination was estimated using ContEst (Broad Institute). Briefly, ContEst quantifies contamination in next-generation sequencing data by identifying homozygous non-reference SNPs in the 1,000 g database and assessing the likelihood of observing alternate alleles at these genomic locations in the sequencing data. Somatic Single

Nucleotide Variant (SNV) calling was performed using Mutect and insetion/deletions (INDELs) were called running Scalpel (scalpel-discovery in–somatic mode). SNVs and INDELs called were further filtered using the following criteria: (i) minimum $\geq$4 variant supporting reads and $\geq$2% variant allele frequency (VAF) supporting the variant, (ii) filtered if present in > 1% population frequency in the 1000g or ExAC database, (iii) filtered through an internally collected list of recurrent sequencing errors ($\geq$3 variant reads and $\leq$20% VAF in at least 30 out of ~2,000 normal samples) on the same sequencing platform. Final list of mutations were annotated using vcf2maf (call VEP for annotation). Tumor mutation burden (TMB) was defined as the total number of missense mutations. In addition, we profiled TMB of these samples by a targeted next-generation sequencing (NGS) panel (Geneseeq) to evaluate its correlation with WES results. Panel TMB was counted by summing all base substitutions and indels in the coding region of targeted genes, including synonymous alterations to reduce sampling noise and excluding known driver mutations as they are over-represented in the panel, as previously described (24).

CNA analysis

CNA analysis in our data was performed using CNVKit (25). Focal level gain and loss were identified if normalized $\log_2$ depth ratio were above 1 or below negative 0.7, respectively. Arm-level CNA was identified if more than 60% of the corresponding chromosome arm was either deleted or amplified. For these 4 regions on chromosome 3p, deletion was called if more than 15% of genes from these segments had copy-number loss. CNAs in immune pathways were called if more than 15% of genes belonging to a given pathway had copy-number loss or gain. Immune pathways and associated genes were defined as these provided by the ImmPort public database.

Statistical analysis

Correlations (such as between WES and panel TMB) were calculated using the Spearman's rank test. Comparisons of proportion between groups were done using the Fisher's exact test. For survival analyses, Kaplan–Meier curves were compared using the log-rank test, and hazard ratios (HR) were calculated by Cox proportional hazards model. A two-sided *P* value of less than 0.05 was considered significant for all tests unless indicated otherwise. For focal CNA analysis, *P* value was corrected for multiple hypothesis testing using the Benjamini–Hochberg method, and FDR values of <0.05 were considered significant. All statistical analyses were done in R (v.3.3.2).

Results

Patient overview

From December 2015, 95 Chinese patients diagnosed with NSCLC have been treated with anti–PD-(L)1 monotherapies at Sun Yat-sen University Cancer Center, of whom 78 patients were included in the final analysis with evaluable radiological results, primary tumor [formalin-fixed paraffin-embedded (FFPE) sections of resected tumor or biopsy] samples and matched normal blood controls (Supplementary Fig. S1A). Among the 78 patients, tumor samples from 70 patients were profiled using both WES and targeted gene panel (hereafter, panel). The rest 8 patients' samples were tested by either WES (3 patients) or Panel (5 patients) due to limited sample amount (Supplementary Fig. S1B). When both FFPE and biopsy samples were available for the patient, FFPE sample was used in the analysis, given the limited intra-tumoral heterogeneity represented by a single biopsy sample. Biopsy and FFPE samples that originated from the same patient showed a strong correlation in TMB levels (Spearman $\rho = 0.82$, $P < 0.001$; Supplementary Fig. S2A), and no significant difference was observed in median TMB (Supplementary Fig. S2B). The clinical characteristics of this cohort were summarized in Table 1 with details in Supplementary Table S1. Almost all patients (99%) were stage IV at diagnosis with a median age of 54 years old at the time of treatment initiation. 60% of the patients had adenocarcinoma, followed by squamous carcinoma (31%). Half of the patients had smoking history with more males in the cohort (68% vs. 32%). 94% of patients were administrated with three different anti–PD-1 therapies, respectively, and the remaining patients underwent PD-L1 blockade. 23% of the patients harbored actionable driver alterations in *EGFR*, *ALK*, and *ERBB2*.

Table 1. Baseline clinical characteristics

Characteristic	All patients ($N = 78$)
Median age (range)	54 (28–73)
Sex – No. (%)	
Male	53 (68%)
Female	25 (32%)
Pathological Type – No. (%)	
Adenocarcinoma	47 (60%)
Squamous carcinoma	24 (31%)
Others	7 (9%)
Stage – No. (%)	
III	1 (1%)
IV	77 (99%)
Immunotherapies – No. (%)	
Anti–PD-1	73 (94%)
Anti–PD-L1	5 (6%)
Smoking Status – No. (%)	
Current or former smoker	38 (49%)
Never smoker	40 (51%)
Actionable Driver Mutations – No. (%)	
EGFR: 19del/L858R/20ins/G719A	8 (10%)
ALK Fusion	3 (4%)
ERBB2 Activating	7 (9%)

Abbreviations: PD-1, programmed cell death protein-1; PD-L1, programmed death-ligand 1.

ORR was 17.9%, which is consistent with previous reports on patients with NSCLC who progressed on prior treatments (6, 7, 11, 26). The overall rate of DCB, defined as patients who achieved partial response (PR) or had prolonged stable disease (SD) for at least 6 months, was 26.9%, and the remaining were classified as non-durable benefit (NDB) group. The median progression-free survival (mPFS) was 63 days. No difference in PFS was observed among the four anti–PD-(L)1 agents (Supplementary Fig. S3).

Tumor mutation burden correlated with immunotherapy benefit

The median TMB was 87 mutations (range, 4–1,528) and 7 mutations (range 0–71), as assessed by WES and Panel, respectively. In comparison with other studies (18, 19), our median TMB was relatively lower, which might result from a higher rate of never-smokers in our cohort. Of the 70 patients whose tumor samples were profiled using both WES and Panel, a strong correlation of TMB analyzed by both methods was observed (Spearman $\rho = 0.81$, $P < 0.001$; Fig. 1A). Based on

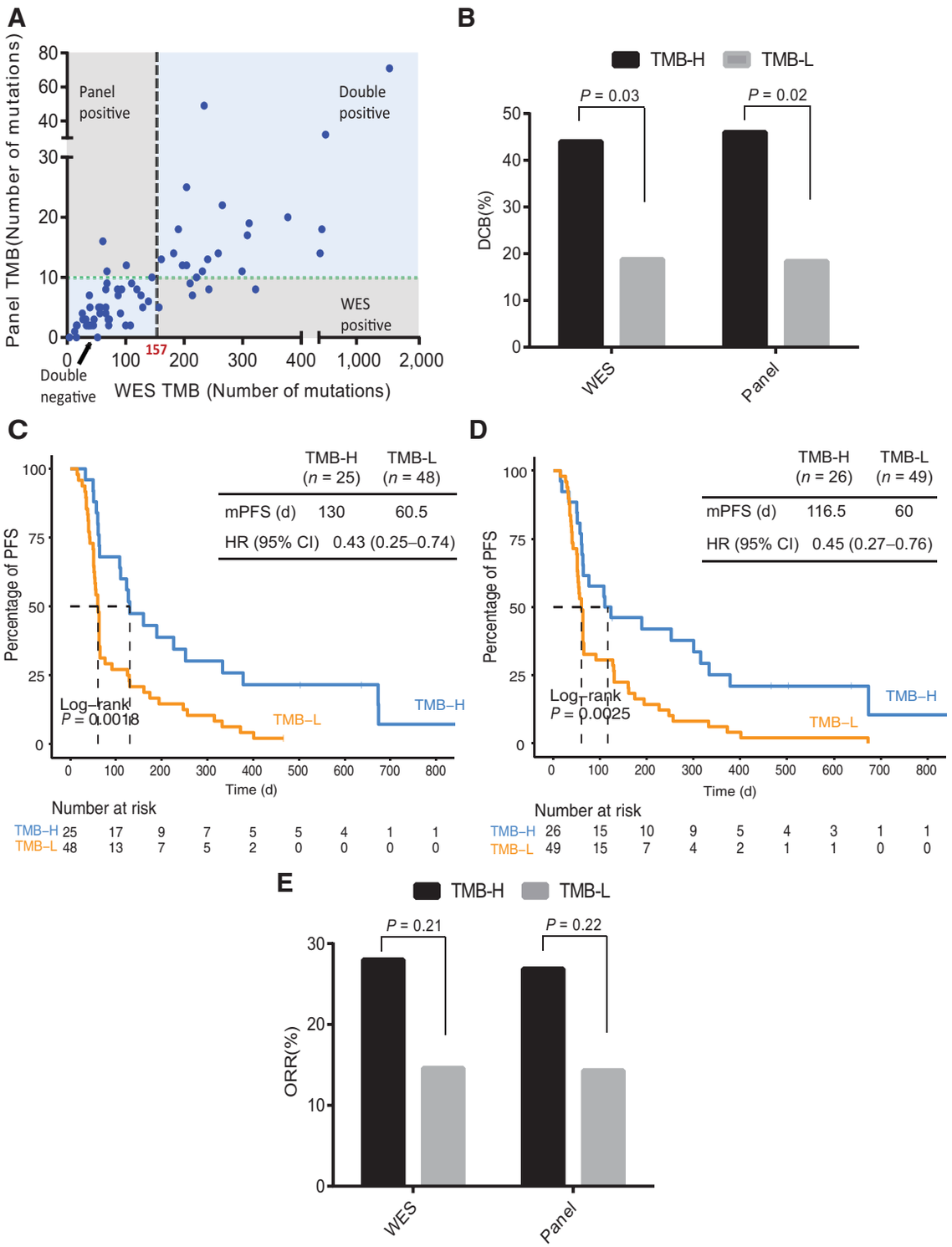

Figure 1.

TMB assessed by WES or targeted NGS correlate with immunotherapy response. **A,** Correlation between TMB assessed by WES and targeted NGS ($n = 70$, Spearman $\rho = 0.81$). **B,** High TMB, estimated by WES or targeted NGS, significantly enrich for patients who experienced durable clinical benefit (DCB). **C** and **D,** Improved progression-free survival (PFS) in patients with high TMB, as assessed by (**C**) WES and (**D**) targeted NGS. **E,** A trend toward increased objective response rate (ORR) is also observed in patients with high TMB.

WES-assessed TMB results, DCB rate and mPFS were both significantly increased in patients with high TMB (top 33%, cutoff = 157 mutations; DCB rate, 44.0% vs. 18.8%, Fisher's exact test $P = 0.03$; mPFS, 130 vs. 60.5 days, log rank $P = 0.0018$, HR, 0.43; 95% confidence interval (CI), 0.25–0.74; Fig. 1B and C]. Similarly, results from Panel assessment also demonstrated increased DCB rate and mPFS in TMB-high patients (top 33%, cutoff = 10 mutations; DCB rate, 46.2% vs. 18.4%, Fisher's exact test $P = 0.02$; mPFS, 116 vs. 60 days, log rank $P = 0.0025$, HR, 0.45; 95% CI, 0.27–0.76; Fig. 1B and D). In addition, patients with high TMB assessed by both methods had a trend toward increased ORR rate (WES, 28.0% vs. 14.6%, Fisher's exact test $P = 0.21$; Panel, 26.9% vs. 14.3%, Fisher's exact test $P = 0.22$; Fig. 1E).

No significant difference in TMB (Supplementary Fig. S4A) or PFS (Supplementary Fig. S4B) was observed between patients with adenocarcinoma and squamous cell carcinoma, albeit a trend toward increase in TMB in squamous cell carcinoma, which is consistent with previous studies (27–29).

Individual somatic mutations associated with response to immunotherapy

Although TMB has a relatively good predictive value regarding patients' response, the DCB and ORR rates only reached approximately 46% and 28%, respectively, within the TMB-high cohort, whereas 14% to 18% of TMB-low patients might also respond to immunotherapy. To better stratify patients, we further evaluated individual somatic mutations that may refine the association of TMB status with response to immunotherapy. We focused our analysis on a list of cancer-related genes (http://www.bushmanlab.org/assets/doc/allOnco_Feb2017.tsv), as well as those of immune pathways (ImmPort database; ref. 30). 41 genes with recurrent mutations (occurred in at least 6 patients) were examined for associations with rates of DCB and ORR, or PFS. The top 15 most common recurrent genes were shown in Fig. 2, top. About half of the patients harbored *TP53* alterations, although no correlation with response was observed. Activating mutations in *EGFR*, *ERBB2*, and *KRAS* were identified in 12%, 11%, and 8% of patients, respectively, in a mutually exclusive manner.

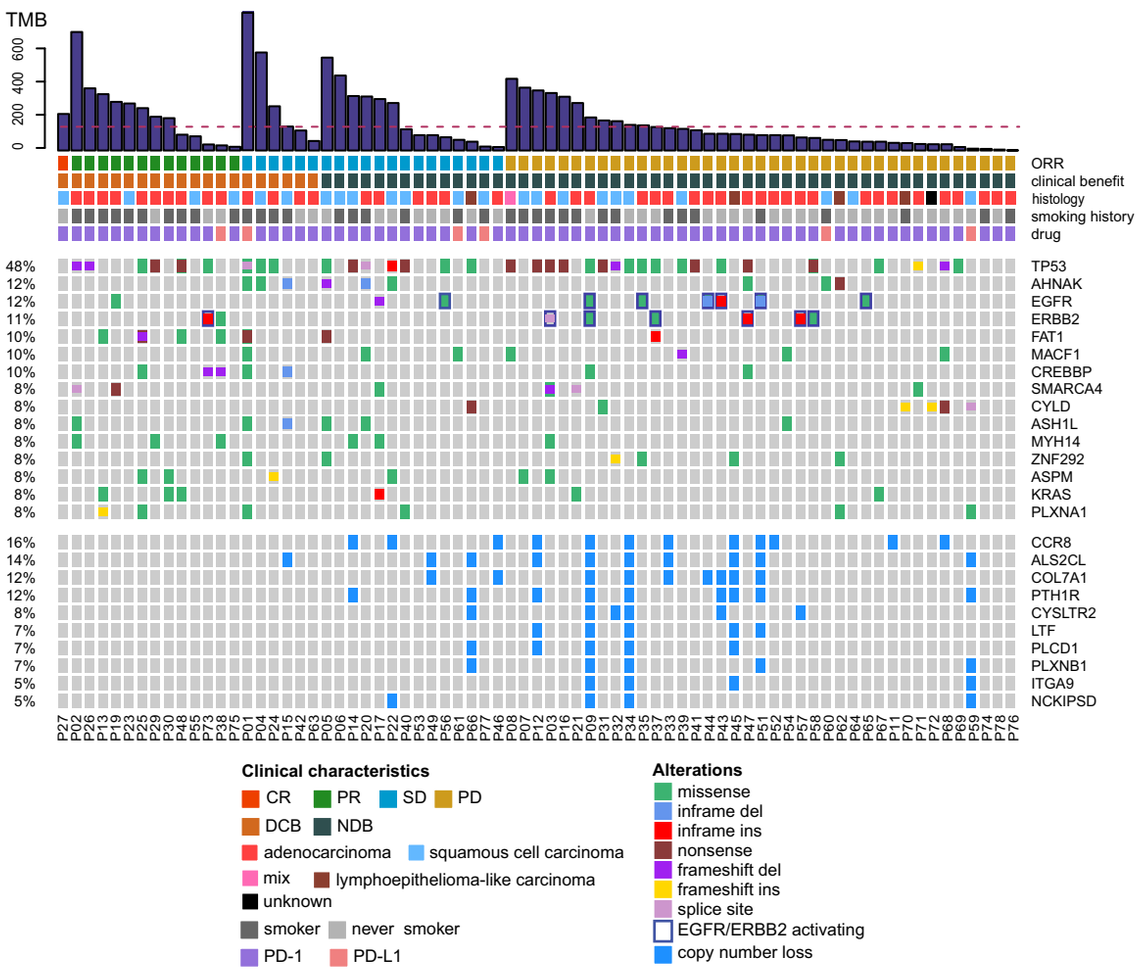

Figure 2.
Distribution of genetic variations associated with anti-PD-(L)1 therapy response. Distributions of individual gene mutations (top) and copy-number variations (bottom) in the study cohort as assessed by WES. Each column represents one patient. Clinical characteristics and WES-assessed TMB values of each patient were shown at the top. PR, partial response; SD, stable disease; PD, progressive disease; CR, complete response; DCB, durable clinical benefit; NDB, non-durable benefit.

Consistent with previous reports (17–19, 31), activating mutations in *EGFR* were exclusively identified in the NDB group (Fig. 2), which were associated with reduced mPFS compared with the rest of the cohort (Supplementary Fig. S5A). Interestingly, activating mutations in *ERBB2* were also over-represented in the NDB group, with only 14% ORR and DCB rates (1 out of 7 patients; Fig. 2). Likewise, these patients had reduced mPFS compared with the rest of the cohort (Supplementary Fig. S5B), although the association between *ERBB2* mutations and mPFS became marginally insignificant ($P = 0.054$) after adjusting for TMB as 2 out of 7 patients were in the TMB-high group (Supplementary Table S2). Considering that *EGFR* and *ERBB2* encode closely related ErbB family receptor tyrosine kinases and they were mutated in almost exclusively different patients, we grouped the patients with activating mutations in either genes and found that patients with ErbB family mutations had significantly shorter mPFS compared with others (51.0 vs. 70.5 days, log rank $P = 0.0037$, HR, 2.47; 95% CI, 1.32–4.62; Fig. 3A). It is not surprising that all *EGFR*/*ERBB2* mutations were found in patients with adenocarcinoma (Fig. 2). Within the adenocarcinoma subgroup, *EGFR*/*ERBB2* activating mutations remained a negative predictor of response, with lower mPFS than respective wild-type patients (log rank $P = 0.0023$; Supplementary Fig. S5C). Among TMB-high patients, the two ErbB family mutants showed distinctively unfavorable outcome compared with double wild-types (Supplementary Fig. S5D). As activating mutations in cancer-driver genes were often associated with never smokers, and consequently low TMB (32), we assessed the impact of driver mutations (*EGFR*/*ERBB2*/*ALK*) on TMB in non-smokers. Of note, we found no difference in TMB or PFS between driver-negative and driver-positive non-smokers (Supplementary Fig. S5E and S5F).

By contrast, recurrent somatic mutations in *FAT1*, which encodes a cadherin-like tumor suppressor, were significantly enriched in the DCB group (Fig. 2) and were significantly associated with higher DCB and ORR rates compared with wild-type patients (71.4% vs. 22.7%, Fisher's exact test, $P = 0.01$, and 57.1% vs. 15.2%, Fisher's exact test, $P = 0.02$, respectively; Supplementary Fig. S5G and S5H). Although *FAT1* mutations were more commonly observed in adenocarcinoma patients (6 out of 7), the association with DCB remained significant (Fisher exact test $P = 0.0089$; Supplementary Table S3). Importantly, *FAT1* mutation was associated with greater clinical response irrespective of TMB status (Fig. 3C; Supplementary Table S2).

To evaluate the robustness of our results in other NSCLC cohorts and cancer types, we cross-validated our findings using previously published datasets with genomic data and annotated clinical outcomes for patients who received ICIs therapies. The first dataset, by Rizvi and colleagues (18), contains targeted-panel sequencing results of tumors from 240 patients with NSCLC, and the second dataset, by Miao and colleagues (19), is a compilation of WES results of tumor samples from 249 patients enrolled in 8 different studies spanning across multiple cancer types, including NSCLC. We found that *EGFR*/*ERBB2* activating mutations were associated with reduced survival in NSCLC in both datasets (log rank $P = 0.011$; $P = 0.0001$, respectively; Fig. 3D; Supplementary Fig. S6A and S6B; Supplementary Table S2). Combined analysis of the three NSCLC cohorts further confirmed the negative effects of EGFR and ERBB2 activation on patient survival (Supplementary Fig. S6C). In addition, *FAT1* mutations were associated with DCB in Rizvi and colleagues (Fisher's exact test, $P = 0.029$; Fig. 3E). Although this association was not significant in Miao and colleagues due to smaller sample size, 3 out of 4 patients with *FAT1* mutant NSCLC had DCB (Fisher's exact test, $P = 0.336$). Correlation of *FAT1* mutations with DCB, irrespective of TMB status, was also supported by the data from Rizvi and colleagues (Fig. 3F).

Copy-number alterations associated with clinical outcomes to immunotherapy

Acquisition of CNAs is highly common during cancer development, many of which contain genes that play causal roles in oncogenesis (33) and may influence patients' response to immunotherapy. Therefore, we explored the associations of CNAs with ICI response at focal, pathway and chromosomal arm levels. Significant focal CNA events were displayed in Fig. 2 (bottom). Overall, we found that copy number gain events were relatively rare compared with deletions, and none was found to be associated with response to ICIs. At the focal level, we found that loss of tumor-suppressor genes, such as integrin α9 (*ITGA9*) and phospholipase Cδ1 (*PLCD1*), were among the top individual CNA events that significantly correlated with a worse outcome following anti–PD-(L)1 treatment (Fig. 4A; Supplementary Table S4). Specifically, none of the *ITGA9*-loss patients experienced ORR or DCB (Fig. 2). The reduced mPFS in our cohort of patients carrying *ITGA9* loss (36.5 vs. 64 days, HR, 9.09; 95% CI, 2.91–27.78; FDR < 0.05; Fig. 4B) was also recapitulated using the lung cancer data from Miao and colleagues (Supplementary Fig. S7A), as well as other cancer types (Fig. 4C). Validation of CNA results cannot be performed in the Rizvi and colleagues dataset due to their limited genomic coverage of the targeted panel.

Alterations in immune-related genes, through their impact on antigen processing, presentation, MHC expression and immune cell infiltration, among others, have been implicated in resistance to immunotherapy (34). Indeed, when analyzing the impact of copy number loss in immune pathway genes on ICI response (Supplementary Tables S5 and S6), we observed a strong trend of reduced mPFS in patients with interferon-γ (IFN-γ) pathway gene loss compared with other patients (Supplementary Fig. S7B), and significantly shorter mPFS in patients with *JAK2* loss compared with wild-type patients (FDR < 0.05; Supplementary Fig. S7C), which were consistent with previous reports showing copy number loss in IFN-γ pathway genes and *JAK2* as predictive factors of poor immunotherapy response (23, 35, 36). All of the five *JAK2*-loss patients had NDB and low TMB (Fig. 2). Similarly, Loss of *IFNE*, which encodes a type I interferon epsilon, was also associated with poor clinical outcome (FDR < 0.05; Fig. 2; Supplementary Fig. S7D), likely due to its immuno-modulatory functions.

Our data further revealed a strong association between copy-number loss of chemokine receptor (CCR) pathway genes and unfavorable immunotherapy outcome (mPFS, 51 vs. 64.5 days, HR, 2.78; 95% CI, 0.83–9.09; Fig. 4D; Supplementary Table S6). A similar reduction in mPFS was also seen in Miao and colleagues in lung cancer patients with CCR pathway gene loss (Supplementary Fig. S7E) and also across multiple cancer types (Fig. 4E). Importantly, a strong gene-dosage effect of the CCR pathway loss on survival was observed in both our cohort and Miao and colleagues (Fig. 4F and G; Supplementary Fig. S7F), indicating that patients' response to immunotherapy might be a direct result of the combined actions of the CCR pathway.

We also noted that many CCR pathway and tumor-suppressor genes clustered on chromosome 3p (Fig. 4A; Supplementary Fig.

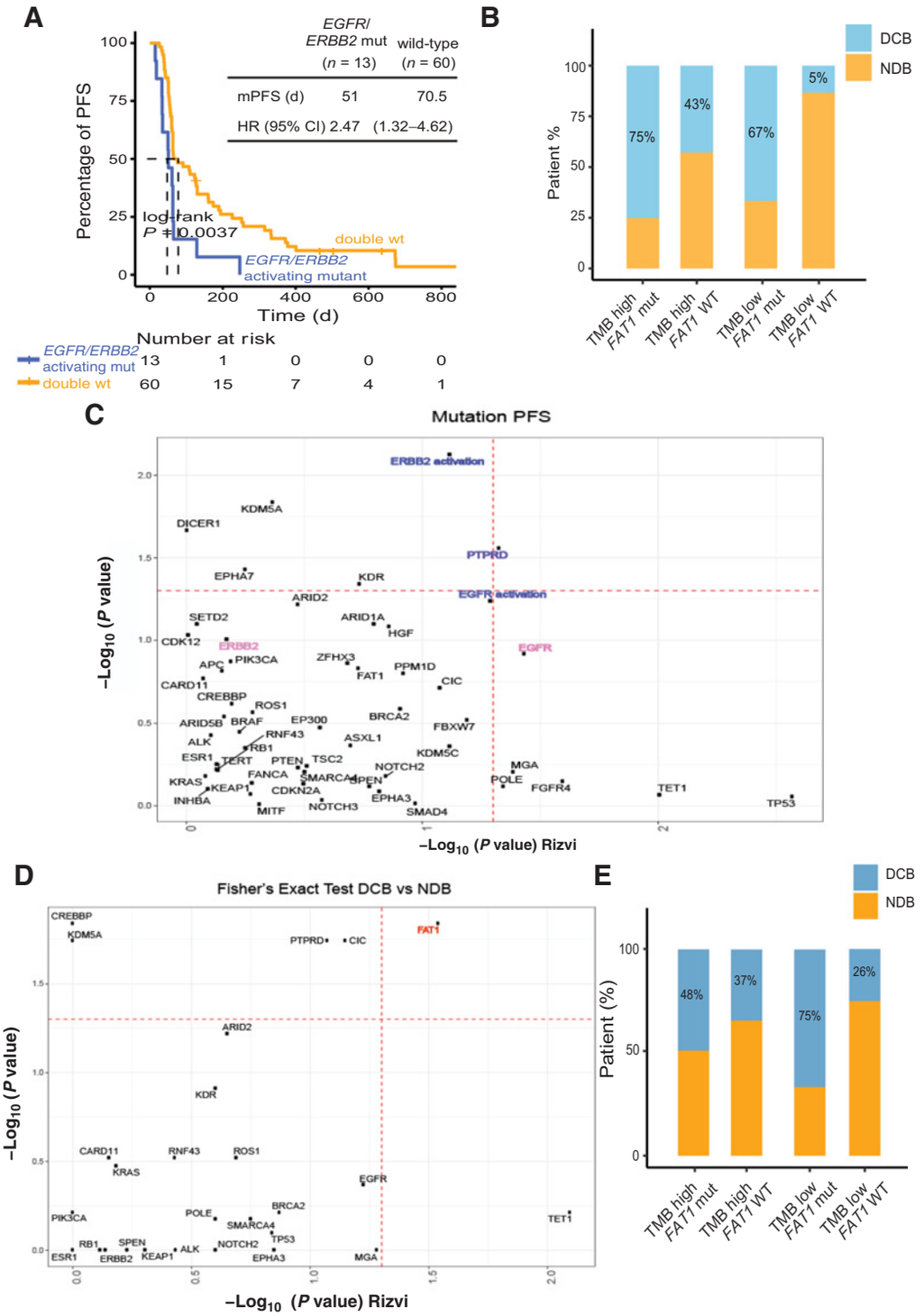

Figure 3.

Individual gene mutations associated with anti–PD-(L)1 therapy response. **A,** Kaplan–Meier estimates of PFS in the full analysis set comparing patients with activating mutations in *EGFR/ERBB2* with their respective wild-type counterparts. **B,** Histograms depicting proportions of patients who experienced DCB in different groups in our study cohort, defined by TMB status and *FAT1* mutations status, as indicated. **C** and **D,** $-\log_{10}(P$ value) comparisons of individual altered genes that are associated with (**C**) PFS and (**D**) DCB versus NDB between our data versus previously published data by Rizvi *et al*. Dashed red lines indicate $P = 0.05$, with individual gene mutations that have $P < 0.05$ in both datasets in the top right corner. **E,** Histograms depicting proportions of patients who experienced DCB in different groups in Rizvi *et al*, defined by TMB status and *FAT1* mutations status, as indicated.

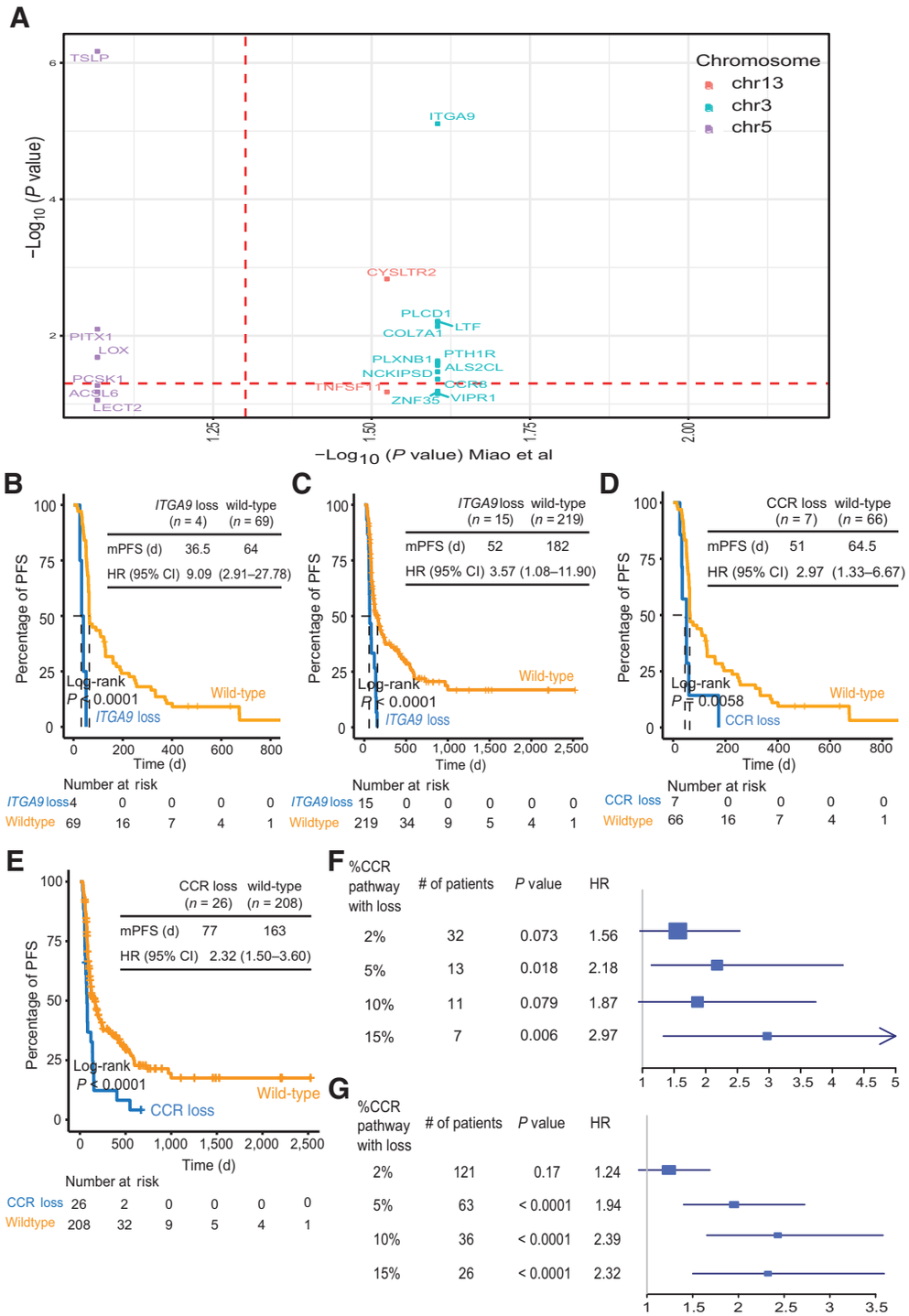

Figure 4.

Focal and immune pathway CNAs associated with anti–PD-(L)1 therapy response. **A,** $-\log_{10}(P$ value) comparisons of individual gene CNAs that are associated with PFS between our own and Miao *et al* datasets. Dashed red lines indicate $P = 0.05$, with individual gene mutations that have $P < 0.05$ in both datasets in the top right corner. Genes were also color coded based on the chromosome they reside on. Note that a majority of individual gene CNAs occurs on chromosome 3. **B** and **C,** Kaplan–Meier estimates of PFS in the full analysis set comparing patients with or without *ITGA9* copy-number loss in (**B**) our data and (**C**) Miao *et al*. full dataset. **D** and **E,** Kaplan–Meier estimates of PFS in the full analysis set comparing patients with or without copy-number loss in the chemokine receptor (CCR) pathway genes in (**D**) our data and (**E**) Miao *et al*. full dataset. **F** and **G,** Forest plots, generated using (**F**) our data and (**G**) Miao *et al.* full dataset, showing gene-dosage dependent effects of CCR pathway loss on PFS hazard ratios.

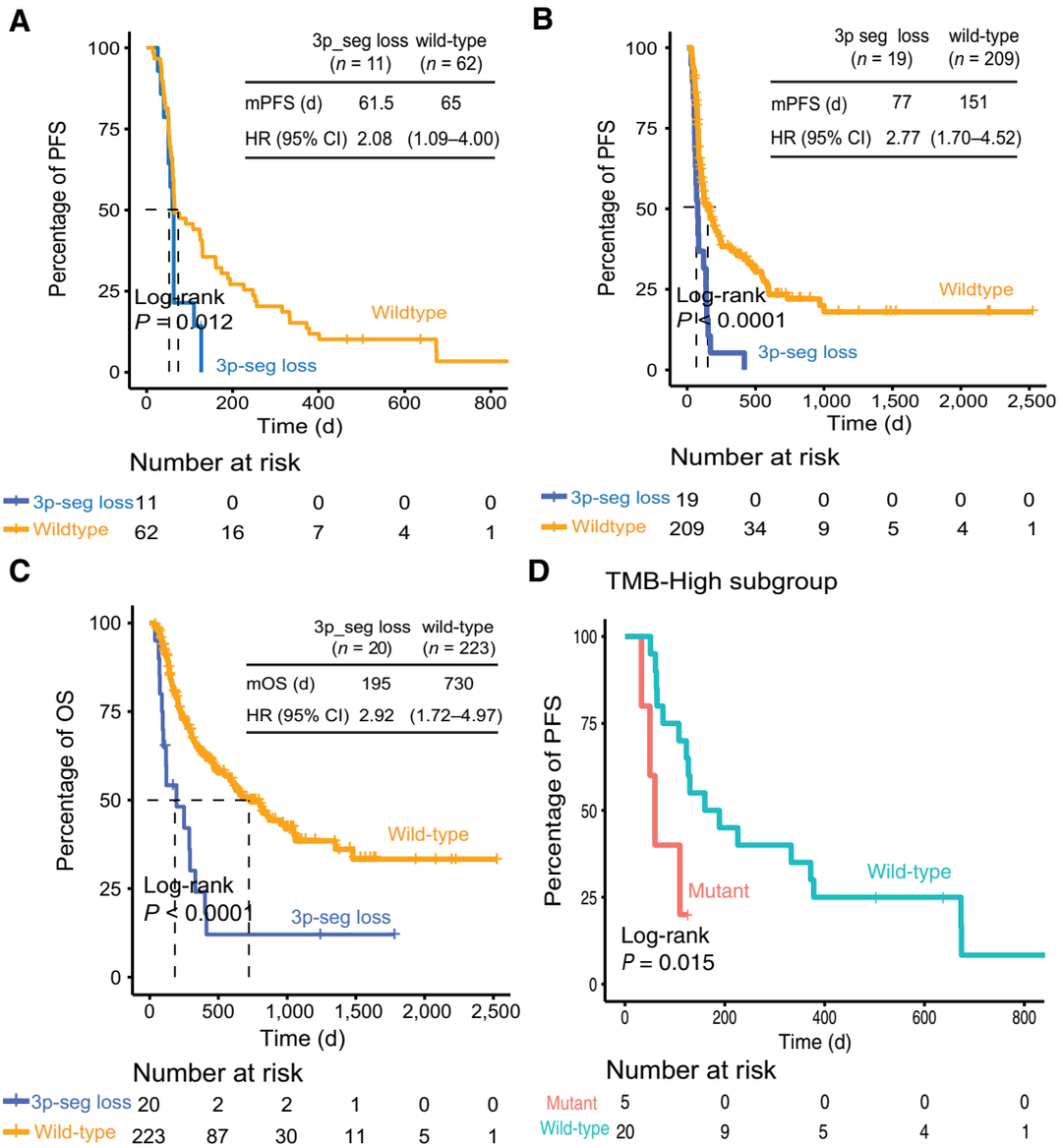

Figure 5.

3p segmental loss, together with *ErbB* mutations, predictive of non-responders to anti–PD-(L)1 therapy. **A** and **B,** Kaplan–Meier estimates of PFS in the full analysis set comparing patients with or without chromosome 3p segmental loss in (**A**) our data and (**B**) Miao *et al*. full dataset. **C,** Kaplan–Meier estimates of OS in Miao *et al*. full analysis set comparing patients with or without chromosome 3p segmental loss. HR denotes hazard ratio; CI denotes confidence interval. Tick indicates censored data. **D,** Kaplan–Meier estimates of PFS in the TMB-H subgroup comparing patients defined by mutant status (mut indicates *EGFR*/*ERBB2*-activating mutations and 3p-segmental loss).

S8A), which is frequently deleted in NSCLC (37, 38). Common eliminated regions on 3p include 3p22 (AP20), 3p21 (CER1, CER2 and LUCA), 3p12 (ROBO1) and 3p14 (FHIT). When examining patients with copy number losses at these 4 regions in our cohort, we observed a significant reduction of survival in these patients compared with wild-type patients (mPFS, 61.5 vs. 65 days; survival rates at day 180, 0% vs. 31%, log rank $P = 0.012$, HR, 2.08; 95% CI, 1.09–4.00; Fig. 5A). The deleterious effect of 3p segment loss on PFS was also evident in Miao and colleagues (Fig. 5B; Supplementary Fig. S8B). Although we were not able to evaluate patients' overall survival (OS) in our cohort, a strong inverse correlation between 3p segmental loss and OS was seen in Miao and colleagues across different cancer types (Fig. 5C). Copy-number loss of specific chromosome 3p segments and chemokine receptor pathway genes remained significant when analyzed in a cox proportional hazard model using histology as a co-variate ($P = 0.016$ and 0.025, respectively; Supplementary Table S2).

Finally, given that ErbB family mutations and multiple CNA events all correlated with poor clinical outcome following anti–PD-(L)1 therapies, we aimed to examine whether combination of these biomarkers could identify non-responders from TMB-high patients. Indeed, pooled analysis of ErbB family mutations and

3p-segment loss events revealed a subset of TMB-high patients who failed to respond to immunotherapies (Fig. 5D). On the other hand, minimal difference in response was observed between mutant and wild-type in the TMB-low subgroup (Supplementary Fig. S8C).

Discussion

Anti–PD-(L)1 therapies have demonstrated improved patient survival in many cancer types, including NSCLCs, although only roughly 20% of patients derived substantial survival benefit. Therefore, there is an urgent need to identify additional biomarkers that can predict response to immunotherapy. In this study, we validated the predictive value of TMB in Chinese patients with NSCLC following immunotherapy and identified additional biomarkers that might help refine the association between TMB and response. Although WES remains the standard method for TMB quantification, increasing evidence has demonstrated that targeted NGS panels, which are of greater clinical utility, can be equally well suited for estimating TMB provided that enough genomic regions were covered (18). Indeed, results from our study confirmed that both sequencing methods could be used to establish the predictive value of TMB in response following ICI treatment. Notwithstanding the increasing popularity of TMB as a predictive biomarker for ICI treatment responses, categorization of patients based on TMB status alone does not suffice an accurate prediction of survival and large gaps remain in the understanding of underlying mechanisms relevant to ICI efficacy. Therefore, exploration of additional tumor characteristics is needed to supplement the predictive power of TMB or PD-L1 expression.

A significant body of evidence exists for the lack of benefit in patients harboring oncogenic mutations in *EGFR* (6, 10, 18, 31). In addition to *EGFR* mutations, our data revealed a previously unrecognized role of *ERBB2* activating mutations in promoting resistance to ICI therapies, which was also observed in datasets from Miao and colleagues and Rizvi and colleagues This result is unsurprising given the similar functions shared by HER2 and EGFR in promoting cell growth and division. On the other hand, mutations in *FAT1* served as a favorable prognostic factor independent of TMB, with DCB rates of 67% to 75% compared with 5% to 43% in *FAT1* wild-type patients. This association was again evident in the validation datasets. Conceivably, other modulating factors of response must exist to account for the approximately 30% of TMB-H/*FAT1* mutant patients who failed to respond, given the complex nature of immune–tumor interactions. Interestingly, a *FAT1*-mutant non-responder in our study carried an additional *ERBB2* activating mutation, which seemed to override the effect of FAT1 on patient response (Fig. 2). Recurrent loss-of-function mutations in *FAT1* were reported in glioblastoma (20.5%), colorectal cancer (7.7%), and head and neck cancer (6.7%). FAT1 is a Drosophila tumor suppressor, which has important functions in regulating the Wnt pathway, as well as the Hippo pathway and consequent inactivation of YAP1 (39–41). Future studies should aim to characterize the role of FAT1 in mediating cancer immune response.

Cancer cells maintain complex and dynamic interactions with the immune system. One well-established mechanism underlying resistance to cancer immunotherapy involves genomic defects in the IFN-γ pathway genes (23, 35, 36), particularly in patients with melanoma treated with anti-CTLA4 therapy. Reduced response to anti–PD-(L)1 therapies was also observed in patients with defective IFN-γ signaling pathway in our study, although to a lesser extent. It is possible that this nuanced difference might be intrinsic to distinct cancer types or ICI agents, in which different sets of immune-modulatory players might be involved. Nonetheless, due to higher resolution at the individual gene level compared with pathways, we showed that CNAs in *JAK2* and *IFNE* were highly associated with lack of benefit in accordance with findings reported by others.

Our data also revealed negative correlations between deletions in specific regions on chromosome 3p with clinical outcome. As many focal deletion events were in close proximity with one another, it is possible that some of them may simply be passenger events adjacent to a driver locus. We noted that important tumor suppressors, such as *ITGA9 and PLCD1*, as well as many CCR pathway genes are enriched in these regions. Similarly, *JAK2*, *IFNE* and the tumor-suppressor *CDKN2A* are all on chromosome 9p. We speculate that *JAK2* and *CDKN2A* might be the primary targets of deletion given their functional significance, which in turn results in the loss of *IFNE* in the process. Whether these are driver CNAs would require further functional analysis, although the deleterious effect of CCR pathway loss was further supported by a gene–dosa`ge-dependent effect on patient response to anti–PD-(L)1 therapies. These findings could potentially be explained by decreased lymphocyte infiltration as shown in another study (42). Although we initially focused on the associations between CNAs and immunotherapy response in NSCLC, these patterns seemed to be present and non-coincidental across multiple cancer types. In addition to the six cancer types analyzed in Miao and colleagues, we also have unpublished data supporting the correlations between CNAs in *ITGA9* and CCR pathway genes and immunotherapy resistance in nasopharyngeal cancers.

Taken together, our study confirmed the utility of large-panel targeted NGS on TMB estimation and demonstrated for the first time the predictive value of TMB in Chinese patients. Furthermore, patients who did not benefit from anti–PD-(L)1 therapies had a higher frequency of genomic alterations in *EGFR*/*ERBB2* and loss of chromosome 3p segments, where several tumor suppressors such as *ITGA9* and many CCR pathway genes are located. By contrast, *FAT1* mutations were enriched in responders. Although the moderate sample size and cohort heterogeneity might limit the conclusions made in this study, our results were validated in two independently published datasets. Therefore, our study provided robust predictive biomarkers of response to ICI therapies, particularly those that consistently distinguished non-responders across multiple cancer types. Thus far, our results, along with other recent studies (17, 18, 43–45), have reported molecular determinants of immunotherapy efficacy, such as inflammatory gene expression profiles, T-cell receptor repertoire, immune cell infiltration, and presence of MHC molecules, in addition to TMB and PD-L1 expression. Further large-scale studies are needed to comprehensively evaluate the generalizability of identified biomarkers in the context of distinct cancer types, independent patient cohorts, and various ICIs regimens. Combinatorial testing of multiple orthogonal biomarkers would provide necessary information to guide personalized immunotherapy.

Disclosure of Potential Conflicts of Interest

No conflicts of interest were disclosed.

Authors' Contributions

Conception and design: W. Fang, Y. Ma, H. Zhao, Y.W. Shao, L. Zhang
Development of methodology: W. Fang, Y. Ma, F. Wang, X. Wu, Y.W. Shao, L. Zhang
Acquisition of data (provided animals, acquired and managed patients, provided facilities, etc.): W. Fang, Y. Ma, S. Hong, Y. Yang, H. Zhao, Y.W. Shao
Analysis and interpretation of data (e.g., statistical analysis, biostatistics, computational analysis): W. Fang, Y. Ma, J.C. Yin, S. Hong, H. Zhou, A. Wang, F. Wang, H. Bao, Y.W. Shao, L. Zhang
Writing, review, and/or revision of the manuscript: W. Fang, Y. Ma, J.C. Yin, S. Hong, H. Zhou, A. Wang, F. Wang, H. Bao, X. Wu, Y. Yang, Y.W. Shao, L. Zhang
Administrative, technical, or material support (i.e., reporting or organizing data, constructing databases): W. Fang, J.C. Yin, F. Wang, L. Zhang
Study supervision: W. Fang, Y. Huang, Y.W. Shao, L. Zhang

Acknowledgments

L. Zhang and work in his laboratory was supported by the National Key R&D Program of China (2016YFC0905500, 2016YFC0905503), as well as the Science and Technology Program of Guangdong (2017B020227001). W. Fang (81772476), S. Hong (81602005), and L. Zhang (81872499) were supported by Chinese National Natural Science Foundation project. S. Hong was also supported by Outstanding Young Talents Program of Sun Yat-sen University Cancer Center (16zxyc04) and Central Basic Scientific Research Fund for Colleges-Young Teacher Training Program of Sun Yat-sen University (17ykpy81).

The costs of publication of this article were defrayed in part by the payment of page charges. This article must therefore be hereby marked *advertisement* in accordance with 18 U.S.C. Section 1734 solely to indicate this fact.

Received February 17, 2019; revised April 4, 2019; accepted May 8, 2019; published first May 13, 2019.

References

1. Topalian SL, Taube JM, Anders RA, Pardoll DM. Mechanism-driven biomarkers to guide immune checkpoint blockade in cancer therapy. Nat Rev Cancer 2016;16:275–87.
2. Samstein RM, Lee CH, Shoushtari AN, Hellmann MD, Shen R, Janjigian YY, et al. Tumor mutational load predicts survival after immunotherapy across multiple cancer types. Nat Genet 2019;51:202–206.
3. Garon EB, Rizvi NA, Hui R, Leighl N, Balmanoukian AS, Eder JP, et al. Pembrolizumab for the treatment of non–small cell lung cancer. N Engl J Med 2015;372:2018–28.
4. Le DT, Uram JN, Wang H, Bartlett BR, Kemberling H, Eyring AD, et al. PD-1 blockade in tumors with mismatch-repair deficiency. N Engl J Med 2015; 372:2509–20.
5. Barlesi F, Vansteenkiste J, Spigel D, Ishii H, Garassino M, de Marinis F, et al. Avelumab versus docetaxel in patients with platinum-treated advanced non-small-cell lung cancer (JAVELIN Lung 200): an open-label, randomised, phase 3 study. Lancet Oncol 2018;19:1468–79.
6. Borghaei H, Paz-Ares L, Horn L, Spigel DR, Steins M, Ready NE, et al. Nivolumab versus docetaxel in advanced nonsquamous non–small cell lung cancer. N Engl J Med 2015;373:1627–39.
7. Brahmer J, Reckamp KL, Baas P, Crino L, Eberhardt WE, Poddubskaya E, et al. Nivolumab versus docetaxel in advanced squamous-cell non–small cell lung cancer. N Engl J Med 2015;373:123–35.
8. Carbone DP, Reck M, Paz-Ares L, Creelan B, Horn L, Steins M, et al. First-line nivolumab in stage IV or recurrent non–small cell lung cancer. N Engl J Med 2017;376:2415–26.
9. Garassino MC, Cho B-C, Kim J-H, Mazières J, Vansteenkiste J, Lena H, et al. Durvalumab as third-line or later treatment for advanced non–small cell lung cancer (ATLANTIC): an open-label, single-arm, phase 2 study. Lancet Oncol 2018;19:521–36.
10. Herbst RS, Baas P, Kim D-W, Felip E, Pérez-Gracia JL, Han J-Y, et al. Pembrolizumab versus docetaxel for previously treated, PD-L1-positive, advanced non–small cell lung cancer (KEYNOTE-010): a randomised controlled trial. Lancet 2016;387:1540–50.
11. Rittmeyer A, Barlesi F, Waterkamp D, Park K, Ciardiello F, von Pawel J, et al. Atezolizumab versus docetaxel in patients with previously treated non–small cell lung cancer (OAK): a phase 3, open-label, multicentre randomised controlled trial. Lancet 2017;389:255–65.
12. Reck M, Rodriguez-Abreu D, Robinson AG, Hui R, Csoszi T, Fulop A, et al. Pembrolizumab versus chemotherapy for PD-L1-positive non-small-cell lung cancer. N Engl J Med 2016;375:1823–33.
13. Hellmann MD, Ciuleanu TE, Pluzanski A, Lee JS, Otterson GA, Audigier-Valette C, et al. Nivolumab plus ipilimumab in lung cancer with a high tumor mutational burden. N Engl J Med 2018;378:2093–104.
14. Hellmann MD, Callahan MK, Awad MM, Calvo E, Ascierto PA, Atmaca A, et al. Tumor mutational burden and efficacy of nivolumab monotherapy and in combination with ipilimumab in small-cell lung cancer. Cancer Cell 2018;33:853–61e4.
15. Rizvi NA, Hellmann MD, Snyder A, Kvistborg P, Makarov V, Havel JJ, et al. Mutational landscape determines sensitivity to PD-1 blockade in non-small cell lung cancer. Science 2015;348:124–8.
16. Yarchoan M, Hopkins A, Jaffee EM. Tumor mutational burden and response rate to PD-1 inhibition. N Engl J Med 2017;377:2500–1.
17. Hellmann MD, Nathanson T, Rizvi H, Creelan BC, Sanchez-Vega F, Ahuja A, et al. Genomic features of response to combination immunotherapy in patients with advanced non-small-cell lung cancer. Cancer Cell 2018;33: 843–52.
18. Rizvi H, Sanchez-Vega F, La K, Chatila W, Jonsson P, Halpenny D, et al. Molecular determinants of response to anti-programmed cell death (PD)-1 and anti-programmed death-ligand 1 (PD-L1) blockade in patients with non-small-cell lung cancer profiled with targeted next-generation sequencing. J Clin Oncol 2018;36:633–41.
19. Miao D, Margolis CA, Vokes NI, Liu D, Taylor-Weiner A, Wankowicz SM, et al. Genomic correlates of response to immune checkpoint blockade in microsatellite-stable solid tumors. Nat Genet 2018;50:1271–81.
20. McGranahan N, Furness AJ, Rosenthal R, Ramskov S, Lyngaa R, Saini SK, et al. Clonal neoantigens elicit T cell immunoreactivity and sensitivity to immune checkpoint blockade. Science 2016;351:1463–9.
21. Skoulidis F, Goldberg ME, Greenawalt DM, Hellmann MD, Awad MM, Gainor JF, et al. STK11/LKB1 mutations and PD-1 inhibitor resistance in KRAS-mutant lung adenocarcinoma. Cancer Discov 2018;8:822–35.
22. Horn S, Leonardelli S, Sucker A, Schadendorf D, Griewank KG, Paschen A. Tumor CDKN2A-associated JAK2 loss and susceptibility to immunotherapy resistance. J Natl Cancer Inst 2018;110:677–81.
23. Gao J, Shi LZ, Zhao H, Chen J, Xiong L, He Q, et al. Loss of IFNgamma pathway genes in tumor cells as a mechanism of resistance to anti-CTLA-4 therapy. Cell 2016;167:397–404.
24. Chalmers ZR, Connelly CF, Fabrizio D, Gay L, Ali SM, Ennis R, et al. Analysis of 100,000 human cancer genomes reveals the landscape of tumor mutational burden. Genome Med 2017;9.
25. Talevich E, Shain AH, Botton T, Bastian BC. CNVkit: genome-wide copy number detection and visualization from targeted DNA sequencing. PLoS Comput Biol 2016;12:e1004873.
26. Fehrenbacher L, Spira A, Ballinger M, Kowanetz M, Vansteenkiste J, Mazieres J, et al. Atezolizumab versus docetaxel for patients with previously treated non-small-cell lung cancer (POPLAR): a multicentre, open-label, phase 2 randomised controlled trial. Lancet 2016;387: 1837–46.
27. Cancer Genome Atlas Research N. Comprehensive genomic characterization of squamous cell lung cancers. Nature 2012;489:519–25.
28. Cancer Genome Atlas Research N. Comprehensive molecular profiling of lung adenocarcinoma. Nature 2014;511:543–50.
29. Hendriks LE, Rouleau E, Besse B. Clinical utility of tumor mutational burden in patients with non-small cell lung cancer treated with immunotherapy. Transl Lung Cancer Res 2018;7:647–60.
30. Bhattacharya S, Dunn P, Thomas CG, Smith B, Schaefer H, Chen J, et al. ImmPort, toward repurposing of open access immunological assay data for translational and clinical research. Sci Data 2018;5:180015.
31. Gainor JF, Shaw AT, Sequist LV, Fu X, Azzoli CG, Piotrowska Z, et al. EGFR mutations and ALK rearrangements are associated with low response rates

to PD-1 pathway blockade in non-small cell lung cancer: a retrospective analysis. Clin Cancer Res 2016;22:4585–93.
32. Govindan R, Ding L, Griffith M, Subramanian J, Dees ND, Kanchi KL, et al. Genomic landscape of non-small cell lung cancer in smokers and never-smokers. Cell 2012;150:1121–34.
33. Beroukhim R, Mermel CH, Porter D, Wei G, Raychaudhuri S, Donovan J, et al. The landscape of somatic copy-number alteration across human cancers. Nature 2010;463:899–905.
34. Sharma P, Hu-Lieskovan S, Wargo JA, Ribas A. Primary, adaptive and acquired resistance to cancer immunotherapy. Cell 2017;168: 707–23.
35. Zaretsky JM, Garcia-Diaz A, Shin DS, Escuin-Ordinas H, Hugo W, Hu-Lieskovan S, et al. Mutations associated with acquired resistance to PD-1 blockade in melanoma. N Engl J Med 2016;375:819–29.
36. Shin DS, Zaretsky JM, Escuin-Ordinas H, Garcia-Diaz A, Hu-Lieskovan S, Kalbasi A, et al. Primary resistance to PD-1 blockade mediated by JAK1/2 mutations. Cancer Discov 2017;7:188–201.
37. Zabarovsky ER, Lerman MI, Minna JD. Tumor suppressor genes on chromosome 3p involved in the pathogenesis of lung and other cancers. Oncogene 2002;21:6915–35.
38. Kok K, Naylor SL, Buys CH. Deletions of the short arm of chromosome 3 in solid tumors and the search for suppressor genes. Adv Cancer Res 1997;71: 27–92.
39. Morris LG, Kaufman AM, Gong Y, Ramaswami D, Walsh LA, Turcan S, et al. Recurrent somatic mutation of FAT1 in multiple human cancers leads to aberrant Wnt activation. Nat Genet 2013;45:253–61.
40. Martin D, Degese MS, Vitale-Cross L, Iglesias-Bartolome R, Valera JLC, Wang Z, et al. Assembly and activation of the Hippo signalome by FAT1 tumor suppressor. Nat Commun 2018;9:2372.
41. Li Z, Razavi P, Li Q, Toy W, Liu B, Ping C, et al. Loss of the FAT1 tumor suppressor promotes resistance to CDK4/6 inhibitors via the hippo pathway. Cancer Cell 2018;34:893–905.
42. Siemers NO, Holloway JL, Chang H, Chasalow SD, Ross-MacDonald PB, Voliva CF, et al. Genome-wide association analysis identifies genetic correlates of immune infiltrates in solid tumors. PLoS ONE 2017;12: e0179726.
43. Roh W, Chen PL, Reuben A, Spencer CN, Prieto PA, Miller JP, et al. Integrated molecular analysis of tumor biopsies on sequential CTLA-4 and PD-1 blockade reveals markers of response and resistance. Sci Transl Med 2017;9.
44. Riaz N, Havel JJ, Makarov V, Desrichard A, Urba WJ, Sims JS, et al. Tumor and microenvironment evolution during immunotherapy with nivolumab. Cell 2017;171:934–49e16.
45. McGranahan N, Rosenthal R, Hiley CT, Rowan AJ, Watkins TBK, Wilson GA, et al. Allele-specific HLA loss and immune escape in lung cancer evolution. Cell 2017;171:1259–71e11.